The Plant Cell, Vol. 22: 1733–1748, June 2010, www.plantcell.org © 2010 American Society of Plant Biologists

MOTHER OF FT AND TFL1 Regulates Seed Germination through a Negative Feedback Loop Modulating ABA Signaling in *Arabidopsis* [C][W]

Wanyan Xi,[1] Chang Liu,[1] Xingliang Hou, and Hao Yu[2]

Department of Biological Sciences and Temasek Life Sciences Laboratory, National University of Singapore, 117543, Singapore

Abscisic acid (ABA) and gibberellin (GA) are two antagonistic phytohormones that regulate seed germination in response to biotic and abiotic environmental stresses. We demonstrate here that *MOTHER OF FT AND TFL1* (*MFT*), which encodes a phosphatidylethanolamine-binding protein, regulates seed germination via the ABA and GA signaling pathways in *Arabidopsis thaliana*. *MFT* is specifically induced in the radical-hypocotyl transition zone of the embryo in response to ABA, and *mft* loss-of-function mutants show hypersensitivity to ABA in seed germination. In germinating seeds, *MFT* expression is directly regulated by ABA-INSENSITIVE3 (ABI3) and ABI5, two key transcription factors in ABA signaling pathway. *MFT* is also upregulated by DELLA proteins in the GA signaling pathway. *MFT* in turn provides negative feedback regulation of ABA signaling by directly repressing *ABI5*. We conclude that during seed germination, *MFT* promotes embryo growth by constituting a negative feedback loop in the ABA signaling pathway.

INTRODUCTION

The first phase transition in the life cycle of higher plants is the switch from embryonic to germinative growth. Seed dormancy blocks the germination process and can be considered an adaptive trait that optimizes the distribution of germination over time (Bewley, 1997). The breakdown of seed dormancy is influenced by both environmental and intrinsic signals (Koornneef et al., 2002), which are mainly mediated by two phytohormones, abscisic acid (ABA) and gibberellin (GA) (Gubler et al., 2005).

ABA is a sesquiterpene hormone that is well known for its physiological role in the processes of seed development and germination as well as plant adaptation to abiotic environmental stresses (Leung and Giraudat, 1998; Finkelstein et al., 2002; Gubler et al., 2005). It has been suggested that ABA inhibits water uptake by preventing cell wall loosening of the embryo during seed germination, indicating that ABA is able to reduce embryo growth potential (Schopfer and Plachy, 1985). In addition, ABA has also been found to specifically inhibit endosperm rupture rather than testa (i.e., seed coat) rupture (Muller et al., 2006). After extensive efforts made toward understanding the ABA signal transduction, ABA-insensitive (*ABI*) alleles, *ABI1* to *ABI5*, have been identified through screening mutant seeds that could germinate even in the presence of high concentrations of ABA (Koornneef et al., 1984; Finkelstein, 1994). Among these identified *ABI*s, *ABI3* encoding a B3 domain transcription factor and *ABI5* encoding a basic region leucine-zipper (bZIP) transcription factor are necessary for achieving growth arrest when germinating seeds encounter unfavorable conditions (Giraudat et al., 1992; Finkelstein and Lynch, 2000). *ABI5* functions downstream of *ABI3* and is essential to execute the ABA-dependent growth arrest, which occurs after the breakage of seed dormancy but prior to autotrophic growth (Lopez-Molina et al., 2001, 2002). Such growth arrest occurs through recruiting of de novo late embryogenesis programs and confers osmotic tolerance to harsh environmental conditions.

GA is a well-known hormone that promotes seed germination and growth. GA biosynthesis and responses are well coordinated during seed germination (Ogawa et al., 2003). Complex regulatory events in the GA signaling pathway include the crosstalk of GA with other hormones and regulation of genes involved in promoting cell elongation and division (Ogawa et al., 2003). Accumulation of GA is accompanied by reduction of ABA during seed germination, suggesting that GA and ABA play antagonistic roles in this process (Olszewski et al., 2002; Nambara and Marion-Poll, 2005). GA signaling is regulated by a group of repressors collectively called DELLA proteins, including REPRESSOR OF *ga1-3* (RGA), GA-INSENSITIVE (GAI), and RGA-LIKE1-3 (RGL1-3) (Peng and Harberd, 1997; Dill and Sun, 2001; Lee et al., 2002; Wen and Chang, 2002; Tyler et al., 2004), among which RGL2 appears as the major DELLA factor involved in repressing seed germination (Lee et al., 2002; Tyler et al., 2004). Recent studies have shown that RGL2 stimulates ABA biosynthesis and ABI5 activity, while ABA enhances the *RGL2* expression (Ko et al., 2006; Zentella et al., 2007; Piskurewicz et al., 2008), indicating that RGL2 plays a role in mediating the interaction of GA and ABA during seed germination.

MOTHER OF FT AND TFL1 (*MFT*) is a homolog of *FLOWERING LOCUS T* (*FT*) and *TERMINAL FLOWER 1* (*TFL1*), two regulators with opposite functions in the control of flowering time (Bradley

[1] These authors contributed equally to this work.

[2] Address correspondence to dbsyuhao@nus.edu.sg.

The author responsible for distribution of materials integral to the findings presented in this article in accordance with the policy described in the Instructions for Authors (www.plantcell.org) is: Hao Yu (dbsyuhao@nus.edu.sg).

[C] Some figures in this article are displayed in color online but in black and white in the print edition.

[W] Online version contains Web-only data.

www.plantcell.org/cgi/doi/10.1105/tpc.109.073072

et al., 1997; Kardailsky et al., 1999; Kobayashi et al., 1999). These three genes, together with three additional homologs in *Arabidopsis thaliana*, form the phosphatidylethanolamine-binding protein (PEBP) family, which is evolutionarily conserved in a wide range of species. As loss of *MFT* function does not exhibit observable defects under normal growth conditions (Yoo et al., 2004), its exact biological function is so far unknown. Here, we show that *MFT* is regulated by both ABA and GA pathways during seed germination. In germinating seeds treated with exogenous ABA, *MFT* is upregulated throughout the embryo, most strongly in the cortex and epidermis layers of the radical-hypocotyl transition zone. Seeds of *mft* loss-of-function mutants are hypersensitive to exogenous ABA and exhibit lower germination rate than those of wild-type plants. *MFT* transcription is directly repressed or promoted by ABI3 or ABI5, respectively, while *ABI5* transcription is directly repressed by MFT. Furthermore, the DELLA protein RGL2 directly promotes *MFT* transcription. These results suggest that MFT responds to both ABA and GA signals to control seed germination through mediating negative feedback regulation of ABA signaling.

RESULTS

Phenotypic Characterization of *mft* Mutants in *Arabidopsis*

To examine the expression pattern of *MFT* in *Arabidopsis*, real-time RT-PCR analysis was performed with total RNA extracted from various tissues. *MFT* was expressed highly in developing siliques, moderately in roots and rosette leaves, but weakly in other tissues (Figure 1A). We further dissected siliques and found that *MFT* was preferentially expressed in the developing seeds (Figure 1B), implying a possible role of *MFT* in seed development. To investigate the biological function of *MFT*, two T-DNA insertion alleles of *MFT* in the Columbia-0 (Col-0) background were isolated and designated as *mft-2* and *mft-3*, respectively (Figure 1C). There was no detectable expression of *MFT* in these two homozygous mutant lines, suggesting that *mft-2* and *mft-3* are null alleles (Figure 1C). Under normal growth conditions, homozygous mutants did not show obvious defects. However, in the presence of exogenous ABA, the germination rate of both *mft-2* and *mft-3* seeds was much lower than that of wild-type seeds (Figure 1D), indicating that *MFT* is involved in seed germination in response to ABA. To further assess the role of *MFT* in seed germination, we generated *35S:MFT* transgenic plants. Among 23 lines generated, 16 lines showed higher germination rates, particularly at early stages of seed germination when exogenous ABA was applied (Figure 1E). These results suggest that *MFT* regulates seed germination in response to exogenous ABA. As endogenous ABA levels in *mft-2* seeds after imbibition were comparable to those in the wild type (see Supplemental Figure 1 online), *MFT* may not be directly involved in regulating ABA levels during seed germination.

As ABA induces growth retardation and stomata closure, we further studied whether *MFT* is also involved in regulating other ABA-related physiological responses. After seed germination, both *mft-2* and wild-type seedlings showed similar degrees of growth retardation when exogenous ABA was applied (see Supplemental Figure 2 online). In addition, there was no significant difference in ABA-induced drought tolerance among wild-type plants and the plants with altered *MFT* expression (see Supplemental Figure 3 online), implying that *MFT* might have a specific function in seed germination.

MFT Expression Is Upregulated in Response to ABA

Because the germination of *mft* mutant seeds was hypersensitive to exogenously applied ABA, we examined *MFT* expression levels in response to ABA. Information retrieved from the public *Arabidopsis* microarray database (http://www.bar.utoronto.ca/efp/cgi-bin/efpWeb.cgi) showed that *MFT* was greatly upregulated by ABA (Figure 2A), which is in agreement with our observation that *MFT* expression levels in germinating seeds were gradually elevated along with increased concentrations of ABA (Figure 2B). In situ hybridization revealed that *MFT* was not detectable in the embryo and endosperm of seeds collected 6 h after stratification (see Supplemental Figure 4 online), whereas its upregulation by ABA occurred strongly in the epidermis and cortex and weakly in the provasculature of the radical-hypocotyl transition zone of seeds collected at a later germination stage (Figure 2C). Furthermore, we checked the time-course expression of *MFT* during seed imbibition in two *cyp707a* mutants with high levels of endogenous ABA (Okamoto et al., 2006). Our results demonstrate that *MFT* is also upregulated by endogenous ABA (see Supplemental Figure 5 online).

As high salinity prevents seed germination and stimulates the biosynthesis and accumulation of ABA by activating genes encoding ABA biosynthetic enzymes (Xiong et al., 2002; Xiong and Zhu, 2003), we next investigated whether *MFT* could affect seed germination in response to high salinity. The germination of *mft* seeds was also hypersensitive to NaCl treatment (Figure 2D). In addition, high salt concentrations caused dramatic upregulation of *MFT* expression, which is similar to the ABA effect (Figure 2E). To test if upregulation of *MFT* by high salinity was mediated via the ABA pathway, we treated seeds of *aba1-5* mutants, in which the ABA biosynthesis was severely impaired (Leon-Kloosterziel et al., 1996), with high salinity. Upregulation of *MFT* by high salinity was significantly attenuated in *aba1-5* seeds compared with the wild type (Figure 2E), suggesting that high salinity induces *MFT* expression mainly through the ABA signaling pathway. Furthermore, *MFT* was markedly upregulated in just-germinated seeds compared with geminating seeds treated with high concentrations of ABA (e.g., 10 μM), whereas high salinity upregulated *MFT* in just-germinated seeds to the same level as in geminating seeds (Figure 2F). This demonstrates a cumulative effect of ABA on promoting *MFT* expression during seed germination. Taken together, these results show that *MFT* is upregulated by ABA during seed germination, but loss of *MFT* function results in ABA hypersensitivity, suggesting an antagonistic function of *MFT* against the inhibitory effect of ABA on seed germination.

The Response of *MFT* to ABA Is Directly Mediated by *ABI3* and *ABI5*

Next, we sought to understand the molecular mechanism by which ABA regulates *MFT* expression. *ABI* loci (*ABI1* to

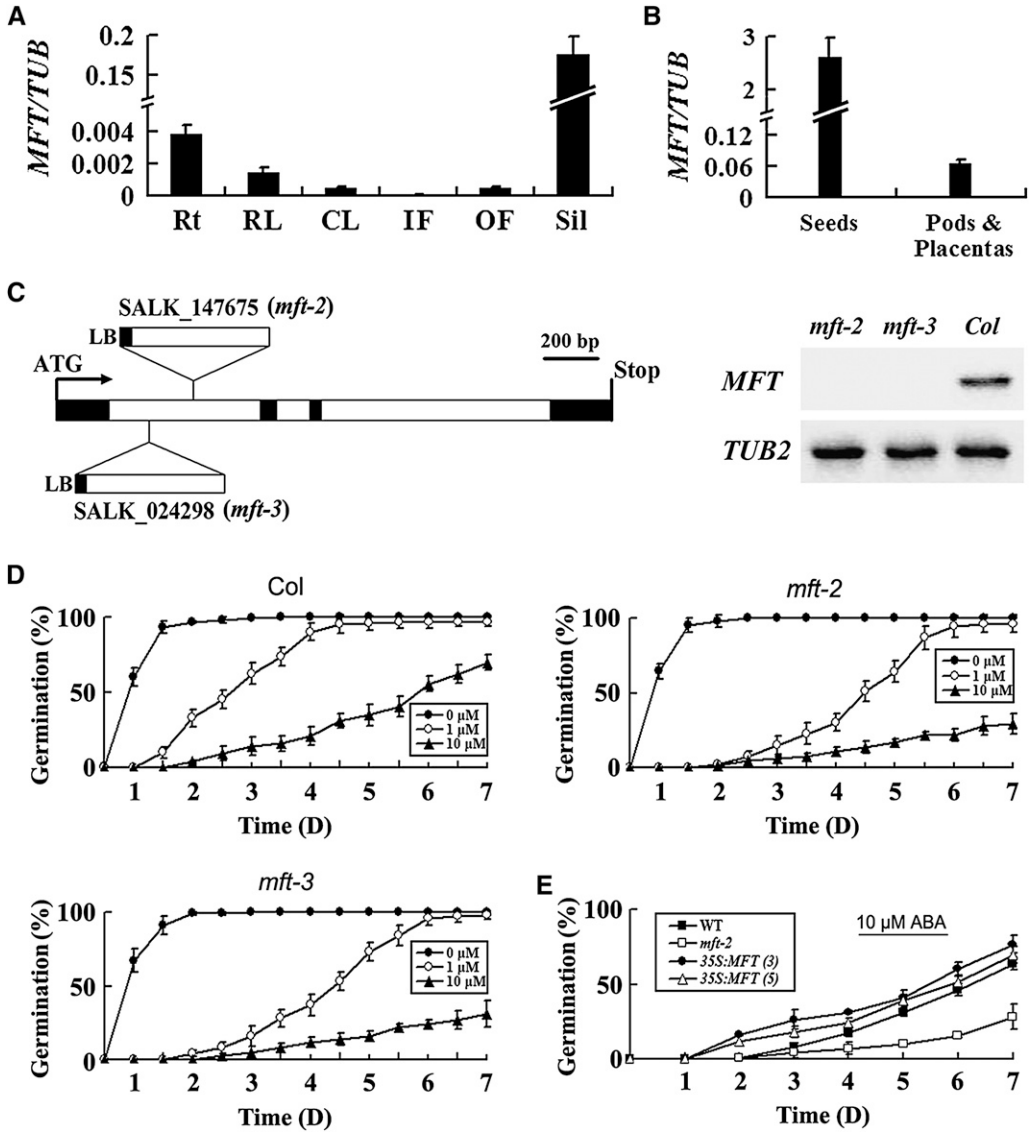

Figure 1. Phenotypic Characterization of *mft* Mutants in *Arabidopsis*.

(A) Quantitative real-time PCR analysis of *MFT* expression in various tissues. Results were normalized against the expression of *TUB2*. Rt, roots; RL, rosette leaves; CL, cauline leaves; IF, inflorescences without open flowers; OF, open flowers; Sil, siliques. Error bars denote SD.

(B) *MFT* expression determined by quantitative real-time PCR in developing siliques dissected into seeds and pods plus placentas. Error bars denote SD.

(C) Schematic diagram indicating the T-DNA insertions in two *mft* loss-of-function mutants, *mft-2* (SALK_147675) and *mft-3* (SALK_024298). Black and white boxes indicate exons and introns of *MFT*, respectively. RT-PCR analysis using a pair of primers flanking the T-DNA insertion sites did not detect *MFT* expression in *mft-2* and *mft-3*, indicating that both of them are null alleles.

(D) Germination phenotype of the wild type, *mft-2*, and *mft-3* treated with different concentrations of ABA (0, 1, and 10 μM). Error bars denote SD.

(E) Germination phenotype of two representative *35S:MFT* lines (3 and 5) in response to 10 μM ABA. Error bars denote SD.

ABI5) have been identified as essential regulators in the ABA signaling network (Koornneef et al., 1984; Finkelstein, 1994). The expression of *ABI3-5* had a similar trend as that of *MFT* in wild-type seeds during imbibition under normal growth conditions (see Supplemental Figure 6 online). We further tested whether these *ABI* genes are involved in the regulation of *MFT* by ABA by examining *MFT* transcript levels in various *abi* mutant seeds in the absence or presence of exogenous ABA. Upregulation of *MFT* by ABA was completely abolished in *abi3-1* and attenuated in *abi5-1* (Figure 3A), suggesting that *ABI3* and *ABI5* mediate the expression of *MFT* in response to ABA. It is noteworthy that with or without ABA treatment, *MFT* expression in *abi3-1* mutant was strikingly higher than that in the wild type (Figure 3A), indicating that *ABI3* negatively regulates *MFT*. On the contrary,

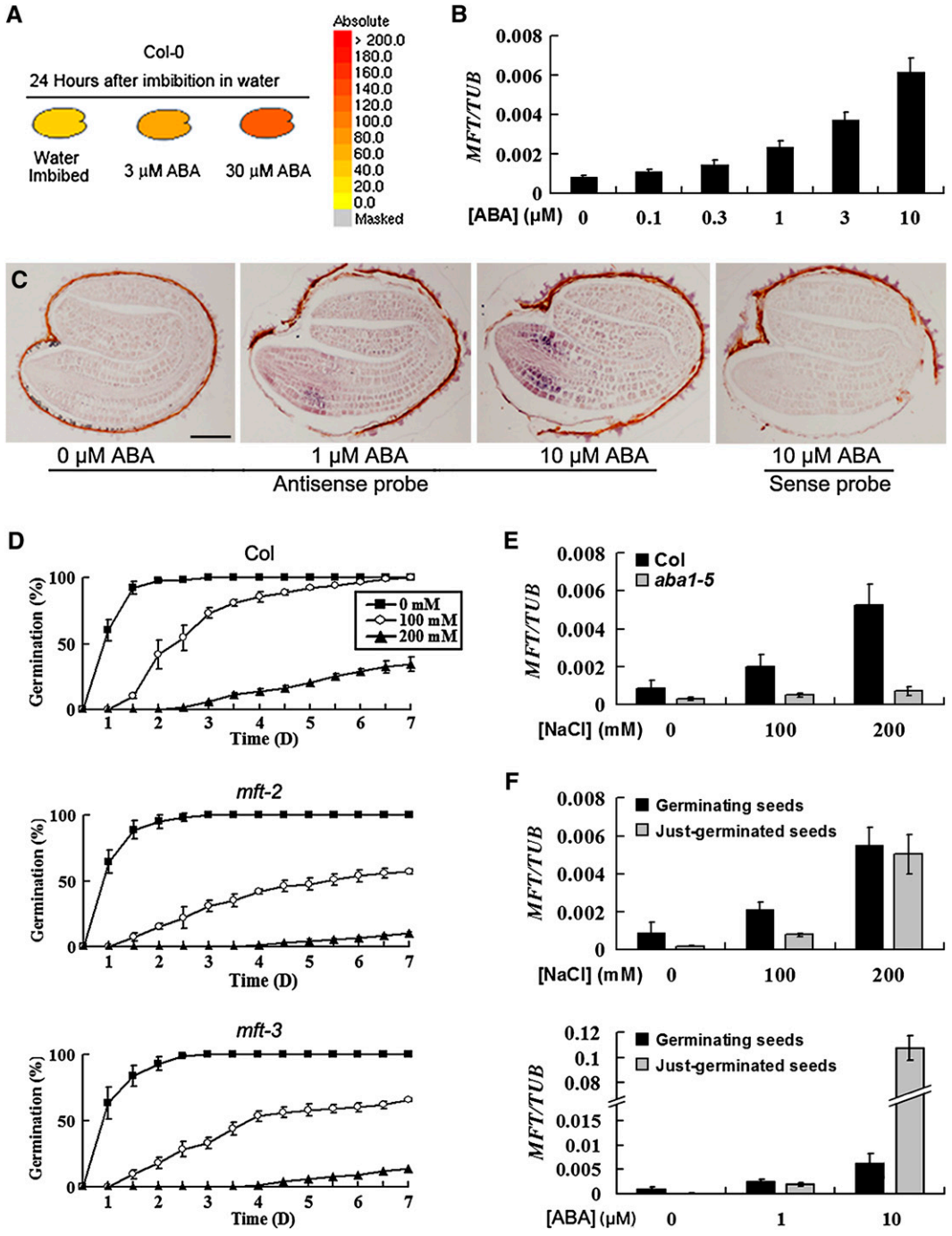

Figure 2. *MFT* Expression Is Upregulated in Response to ABA.

(A) Public microarray data showing upregulation of *MFT* by ABA in germinating seeds (http://www.bar.utoronto.ca/efp/cgi-bin/efpWeb.cgi). The colors from yellow to red indicate the increased absolute signal values of *MFT* expression retrieved from microarray data.

(B) *MFT* expression determined by quantitative real-time PCR in germinating seeds treated with different concentrations of ABA. All seeds were collected 16 h after stratification. Error bars denote SD.

(C) In situ localization of *MFT* in germinating seeds treated with different concentrations of ABA. Seeds without ABA treatment were collected 12 h after stratification, while other seeds treated with 1 and 10 μM ABA were collected 24 h after stratification. These seeds at the same developmental stage were hybridized with the antisense or sense *MFT* probe as indicated. Bar = 100 μm.

(D) Germination phenotype of the wild type, *mft-2*, and *mft-3* treated with different concentrations of NaCl. Error bars denote SD.

(E) *MFT* expression determined by quantitative real-time PCR in wild-type and *aba1-5* germinating seeds treated with different concentrations of NaCl.

MFT expression in *abi5-1* was the lowest among all the mutants treated with high concentrations of ABA (Figure 3A), indicating that *ABI5* promotes *MFT* expression in response to ABA. As the expression levels of *MFT* in *abi3-1 abi5-1* were similar to those in *abi3-1* (Figure 3A), *abi3-1* is epistatic to *abi5-1* in terms of regulating *MFT* expression.

To elucidate the relationship between *ABI3*, *ABI5*, and *MFT*, we created *35S:ABI3-6HA* and *35S:ABI5-6HA* transgenic lines. Low concentrations of ABA significantly lowered the germination rates of these two transgenic plants, which is in agreement with previous reports on *35S:ABI3* and *35S:ABI5* (Lopez-Molina et al., 2001; Zhang et al., 2005), suggesting that both ABI3-6HA and ABI5-6HA fusion proteins are biologically functional (Figure 3B). When *ABI3* was overexpressed, *ABI5* expression was upregulated, whereas *MFT* expression was downregulated in the presence of ABA (Figure 3C). Overexpression of *ABI5* did not affect *ABI3* expression, but did lead to upregulated *MFT* expression in the presence of ABA. As ABA prevents the degradation of ABI3 and ABI5 proteins (Lopez-Molina et al., 2001; Zhang et al., 2005), these results, together with the observation on *MFT* expression in *abi3-1* and *abi5-1*, suggest that ABI3 activity inhibits *MFT* expression, whereas ABI5 has an opposite effect.

We further investigated whether ABI3 and ABI5 directly regulate *MFT* by chromatin immunoprecipitation (ChIP) assays. Promoter analysis identified several putative ABA-responsive elements (ABREs) in the *MFT* promoter. There is a single ABRE and a separate cluster of five ABREs located ~700 bp and 1.7 kb upstream of the initiation codon, respectively (Figure 3D). Since both ABI3 and ABI5 have been shown to regulate ABRE-containing genes (Kim et al., 1997; Ezcurra et al., 1999, 2000; Finkelstein and Lynch, 2000; Kim et al., 2002; Lopez-Molina et al., 2002), the presence of these ABREs in *MFT* promoter implies that ABI3 and ABI5 may directly regulate *MFT* expression. Hence, *35S:ABI3-6HA* and *35S:ABI5-6HA* tagging lines were applied for ChIP assays using four pairs of the primers designed in the *MFT* promoter (MFT-1 to MFT-4). ChIP enrichment revealed that ABI3-6HA was mainly associated with the genomic region near MFT-2, while ABI5-6HA bound to the regions near both MFT-2 and MFT-3 (Figure 3D), suggesting that both ABI3 and ABI5 directly bind to the *MFT* promoter in vivo.

A G-Box Motif Mediates Spatial Regulation of *MFT* in Response to ABA

To further understand how ABA regulates *MFT* through *ABI3* and *ABI5* during seed germination, we generated two *MFT*:β-glucuronidase (*GUS*) constructs, *MFT(P2)-GUS* and *MFT(P6)-GUS*, in which 1.8-kb and 900-bp promoter sequences with six and one ABREs upstream of the translational start site, respectively, were fused with the *GUS* reporter gene (Figure 4A, left panel). The *MFT* coding sequence driven by the 1.8-kb promoter was able to rescue the low germination phenotype of *mft*-2 in response to ABA (see Supplemental Figure 7 online), implying that this promoter region contains essential *cis*-elements required for the regulation of *MFT* expression by ABA. For both *MFT(P2)-GUS* and *MFT(P6)-GUS*, moderate GUS signals were detected in embryos without ABA treatment (Figure 4B). In agreement with *MFT* gene expression profiles (Figures 2A to 2C), when exogenous ABA was applied, GUS staining in these two reporter lines was enhanced throughout the embryos, especially in the radical-hypocotyl transition zone (Figure 4B). While GUS staining was also observed in the seed coat with the endosperm, it was not affected by ABA treatment (data not shown).

Although *MFT(P6)-GUS* showed weaker staining in whole embryos than *MFT(P2)-GUS* in response to ABA, increased GUS staining was specifically observable in the radical-hypocotyl transition zone of *MFT(P6)-GUS* (Figure 4B). This implies that the fived clustered ABREs at ~1.7 kb upstream of the start codon may modulate the extent of *MFT* upregulation throughout the embryo, while the single ABRE close to the start codon may confer the spatial upregulation of *MFT* in the radical-hypocotyl transition zone in response to ABA. We further mutagenized the single ABRE to evaluate its function in response to ABA (Figure 4A, right panel). This ABRE contains one RY repeat that is recognized by ABI3 and one G-box that is recognized by both ABI3 and ABI5 (Kim et al., 1997; Ezcurra et al., 2000). Mutation of the RY motif had no obvious effect on the GUS staining of either *MFT(P2)-GUS* or *MFT(P6)-GUS* in response to ABA, whereas mutation of the G-box motif notably attenuated the responses to ABA (Figure 4B). In particular, upregulation of GUS staining in the radical-hypocotyl transition zone was significantly abolished when the G-box was mutated (Figure 4B). Therefore, the G-box in this single ABRE is essential for upregulating *MFT* expression particularly in the radical-hypocotyl transition zone in response to ABA.

MFT Is Promoted by ABI5 but Suppressed by ABI3

As ChIP assays demonstrated that ABI3 and ABI5 physically bound to the *MFT* promoter, we crossed *MFT:GUS* lines into plants with overexpression or loss of function of *ABI3* and *ABI5* to monitor how they control *MFT* expression in response to ABA during seed germination. Since the germination of *35S:ABI3* and *35S:ABI5* seeds was hypersensitive to low ABA concentrations (Figure 3B) (Lopez-Molina et al., 2001; Zhang et al., 2005), GUS staining of *MFT:GUS* lines in these backgrounds was examined under the treatment of 1 or 3 μM ABA. *MFT(P2)-GUS* exhibited enhanced staining specifically in the radical-hypocotyl transition zone in *35S:ABI5-6HA* in response to ABA, while mutation of the G-box in *MFT(P2)-GUS* did not show any change of GUS staining

Figure 2. (continued).

All seeds were collected 16 h after stratification. Error bars denote SD.

(F) *MFT* expression determined by quantitative real-time PCR in germinating and just-germinated seeds treated with NaCl and ABA. All germinating seeds were collected 16 h after stratification. Seeds with visible protrusion of the radicle tip through all the covering layers were collected as just-germinated seeds. Error bars denote SD.

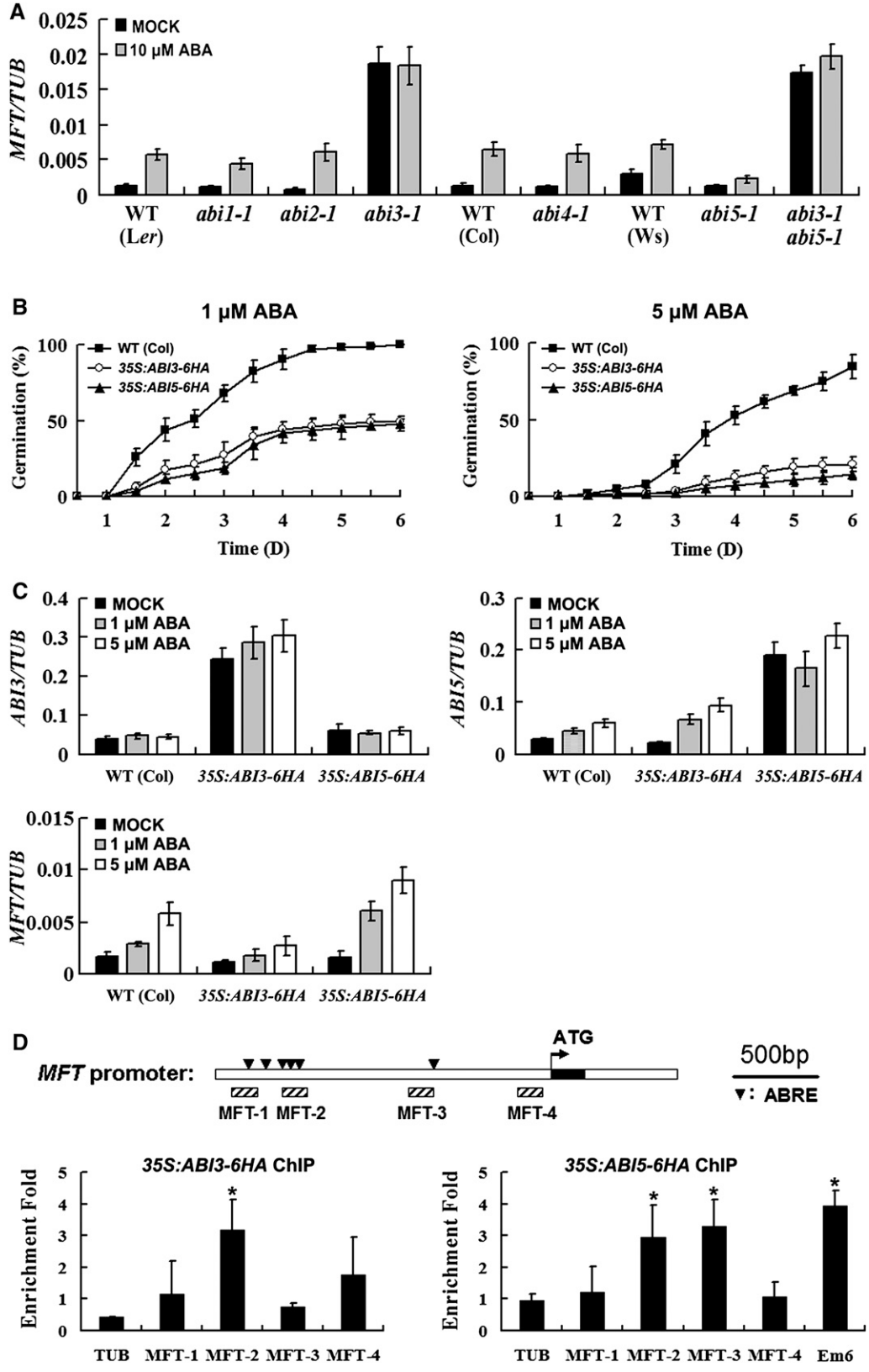

Figure 3. Regulation of *MFT* by ABA Is Mediated by *ABI3* and *ABI5*.

in *35S:ABI5-6HA* (Figure 4C). This finding, together with the ChIP result showing the binding of ABI5 to the promoter region near MFT-3 (Figure 3D), strongly suggests that ABI5 specifically regulates *MFT* expression in the radical-hypocotyl transition zone through the G-box in the ABRE near the start codon. This is confirmed by the observation that *MFT(P2)-GUS* showed decreased GUS staining in the radical elongation zone in *abi5-1* compared with that in wild-type background in response to ABA (Figure 4D).

MFT(P2)-GUS showed slightly reduced GUS staining in *35S:ABI3-6HA* in response to ABA (Figure 4C) but exhibited extraordinarily strong GUS staining in the whole embryo of *abi3-1* independent of ABA treatment (Figure 4D). Further loss of *ABI5* in *abi3-1* had little effect on the intensity of GUS staining in *MFT (P2)-GUS* (Figure 4D). These GUS staining patterns are in agreement with the *MFT* expression in the corresponding transgenic plants or mutants (Figures 3A and 3C), suggesting that ABI3 plays a dominant role in suppressing *MFT* expression in the whole embryo, while ABI5 recognizes the G-box motif to promote *MFT* expression particularly in the radical-hypocotyl transition zone.

MFT Is Regulated by DELLA Proteins

Since GA functions as a major counteracting hormone against ABA to promote both embryo growth potential and endosperm weakening during seed germination (Ogawa et al., 2003; Muller et al., 2006), we asked whether *MFT* is involved in the crosstalk of ABA and GA signaling. We first examined if GA could rescue the low germination rate of *mft-2* caused by ABA. In the presence of 10 μM ABA, increasing the concentration of exogenously applied GA from 1 to 10 μM clearly elevated the germination rate of wild-type seeds but had little effect on the germination of *mft-2* (Figure 5A), implying that *MFT* plays a role in mediating the interaction between ABA and GA signals during seed germination.

We next examined *MFT* expression in the GA-deficient mutant *ga1-3*, which blocks GA biosynthesis (Wilson et al., 1992). *MFT* was highly expressed in *ga1-3* seeds, and exogenously applied GA downregulated *MFT* (Figure 5B), suggesting that GA represses *MFT* expression in seeds. As DELLA proteins are a major family of growth-restricting nuclear proteins mediating the GA effect on growth and RGA and RGL2 are predominant DELLAs involved in seed germination (Lee et al., 2002; Tyler et al., 2004), we tested if DELLA proteins mediate GA regulation of *MFT* by checking *MFT* expression in various *DELLA* mutants in the *ga1-3* background. Loss of RGL2 or RGA activity noticeably reduced *MFT* expression in *ga1-3* with a stronger effect exerted by RGL2 (Figure 5C). In *ga1-3 rga-t2 rgl2-1*, *MFT* expression was much reduced (Figure 5C). Further loss of the activity of other two DELLA proteins, GAI and RGL1, reduced *MFT* expression to a level comparable to that in the wild type (Figure 5C). GA treatment that resulted in the degradation of DELLA proteins considerably downregulated *MFT* expression in almost all the mutants tested except the penta mutant *ga1-3 gai-t6 rga-t2 rgl1-1 rgl2-1*. These results suggest that all DELLA proteins tested contribute to the upregulation of *MFT* in *ga1-3* and that *RGL2* and *RGA* are two major regulators controlling *MFT* expression with the former as the most important regulator.

To examine if DELLA proteins directly modulate *MFT* transcription, we created *ga1-3 rgl2-1 rga-t2 35S:RGL2-GR* inducible lines, in which glucocorticoid receptor (GR) fusion protein could be activated by its ligand dexamethasone (DEX). Application of DEX delayed the germination rate of *ga1-3 rgl2-1 rga-t2 35S:RGL2-GR* (see Supplemental Figure 8 online), suggesting that RGL2-GR is biologically functional in inhibiting seed germination. Combined treatment of *ga1-3 rgl2-1 rga-t2 35S:RGL2-GR* by DEX and cycloheximide, an inhibitor of protein synthesis, resulted in an increase in *MFT* expression. This demonstrates that RGL2 modulates *MFT* expression independently of protein synthesis, indicating that *MFT* may be an immediate target of RGL2 (Figure 5D). To test whether RGL2 could be associated with the *MFT* promoter, we created *35S:RGL2-6HA* lines for ChIP analysis. *35S:RGL2-6HA* was introduced into *ga1-3 rgl2-1*, and the functional lines that mimicked *ga1-3* phenotypes were chosen for further ChIP assays. ChIP enrichment test showed that RGL2-6HA was associated with the region near the MFT-2 fragment (Figure 5E), indicating that RGL2 is directly involved in the regulation of *MFT* expression.

We found that both *ABI3* and *ABI5* expression was elevated in *ga1-3* seeds and that their expression levels in *ga1-3* lacking DELLA proteins (particularly RGL2 and RGA) decreased to the same levels as in wild-type seeds (see Supplemental Figure 9 online). GA treatment of these mutant seeds downregulated

Figure 3. (continued).

(A) *MFT* expression determined by quantitative real-time PCR in wild-type (WT) and various *abi* mutants mock treated or treated with 10 μM ABA. Because *abi3-1* seeds germinated around 14 h after stratification, we collected all germinating seeds 12 h after stratification for comparing *MFT* expression. Error bars denote SD.

(B) Germination phenotype of the wild type, *35S:ABI3-6HA*, and *35S:ABI5-6HA* treated with 1 or 5 μM ABA. Error bars denote SD.

(C) Expression of *ABI3*, *ABI5*, and *MFT* determined by quantitative real-time PCR in germinating seeds of the wild type, *35S:ABI3-6HA*, and *35S:ABI5-6HA* mock treated or treated with 1 or 5 μM ABA. All germinating seeds were collected 16 h after stratification. Error bars denote SD.

(D) ChIP enrichment test showing the binding of ABI3-6HA and ABI5-6HA to the *MFT* promoter. The upstream region and the first intron of *MFT* are represented by white boxes, while the first exon is represented by a black box. The arrowheads in the top panel indicate the sites containing putative ABREs on the *MFT* promoter. Hatched boxes represent the DNA fragments amplified in ChIP assays. ChIP assay results of *35S:ABI3-6HA* and *35S:ABI5-6HA* are shown in the bottom panels. Seeds were sown on Murashige and Skoog (MS) medium supplemented with 10 μM ABA and harvested 16 h after stratification for ChIP assays. *Em6*, which has been identified as a direct target of ABI5 (Lopez-Molina et al., 2002), is used as a positive control for ABI5-6HA ChIP assay. Significant differences in comparison with the enrichment of a *TUB2* fragment are indicated with asterisks ($P < 0.05$, Student's *t* test). Error bars denote SD.

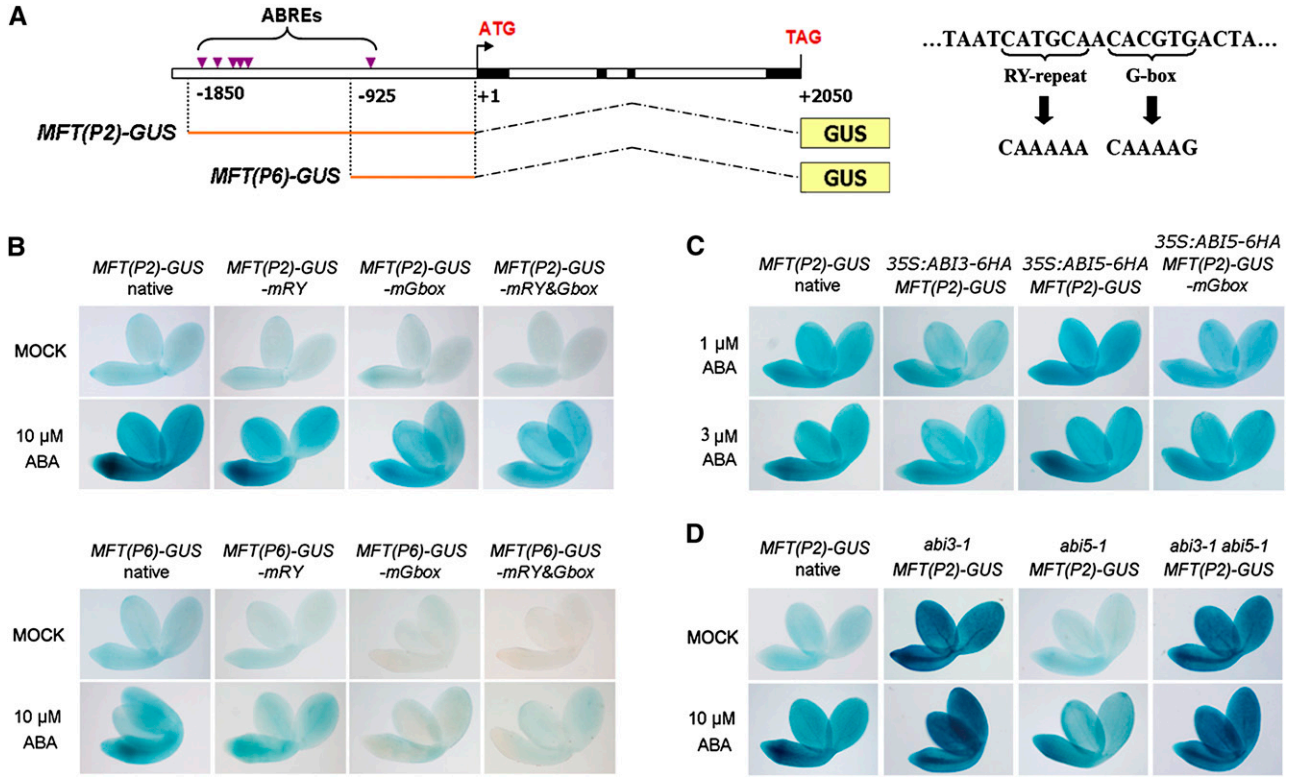

Figure 4. A G-Box Motif in *MFT* Promoter Mediates Spatial Regulation of *MFT* in Response to ABA.

(A) Schematic diagram of *MFT(P2)-GUS* and *MFT(P6)-GUS* constructs where *MFT* 5′ upstream sequences containing ABREs were transcriptionally fused with the *GUS* gene (left panel). The right panel shows the mutagenesis of the RY repeat and the G-box in the ABRE that is located 700 bp upstream of the ATG start codon.

(B) GUS staining in germinating seeds of the transformants containing *MFT(P2)-GUS*, *MFT(P6)-GUS*, and their derived constructs with the mutated RY repeat (mRY) and G-box motif (mGbox). Seeds from T3 homozygous plants with a single insertion of the transgene for each construct were analyzed, and representative images are shown. Germinating seeds mock treated or treated with 10 μM ABA, which were at the same developmental stage, were stained 12 or 24 h after stratification, respectively.

(C) GUS staining in germinating seeds of *MFT(P2)-GUS*, *35S:ABI3-6HA MFT(P2)-GUS*, *35S:ABI5-6HA MFT(P2)-GUS*, and *35S:ABI5-6HA MFT(P2)-GUS-mGbox*. Germinating seeds treated with 1 and 3 μM ABA, which were at the same developmental stage, were stained 24 h after stratification.

(D) GUS staining in germinating seeds of *MFT(P2)-GUS*, *abi3-1 MFT(P2)-GUS*, *abi5-1 MFT(P2)-GUS*, and *abi3-1 abi5-1 MFT(P2)-GUS*. To examine GUS expression in seeds at the same developmental stage, *MFT(P2)-GUS* and *abi5-1 MFT(P2)-GUS* treated with 10 μM ABA were stained 24 h after stratification, while other germinating seeds mock treated or treated with 10 μM ABA were stained 12 h after stratification.

ABI3 and *ABI5* expression to the levels comparable to those of wild-type seeds (see Supplemental Figure 9 online). These results suggest that DELLA proteins promote ABA signaling, which is consistent with the previous findings showing that DELLA proteins stimulate endogenous ABA synthesis (Ko et al., 2006; Zentella et al., 2007; Piskurewicz et al., 2008). Thus, it is likely that in addition to direct regulation of *MFT* expression, RGL2 also indirectly affects *MFT* expression through the ABA signaling pathway.

To understand the biological significance of the upregulation of *MFT* by DELLA proteins, we crossed *mft-2* in Landsberg *erecta* (L*er*) background with *ga1-3* to remove *MFT* activity. As *ga1-3* germinates only upon application of exogenous GA, seed germination was examined in the presence of exogenous GA. Under the same growth conditions, *ga1-3 mft-2* germinated at a lower rate than *ga1-3* in response to GA treatment, especially within 5 d after stratification (Figure 5F). When GA levels are low, DELLA proteins overaccumulate, thus concomitantly promoting *MFT* expression and ABA signaling. The lower germination rate in *ga1-3 mft-2* than in *ga1-3* indicates that when GA biosynthesis is impaired and ABA signaling is stimulated, *MFT* is required to maintain the seed germination potential. In agreement with this, *ga1-3 rgl2-1 mft-2* exhibited a lower germination rate than *ga1-3 rgl2-1* in the absence of exogenous GA (Figure 5G).

MFT Represses *ABI5* Expression during Seed Germination

To understand the mechanism by which *MFT* regulates seed germination, we first checked MFT intracellular localization by examining the localization of gMFT-GFP, in which the *MFT* coding sequence driven by the 1.8-kb promoter was fused with the green fluorescent protein reporter gene. Among 16 *mft-2*

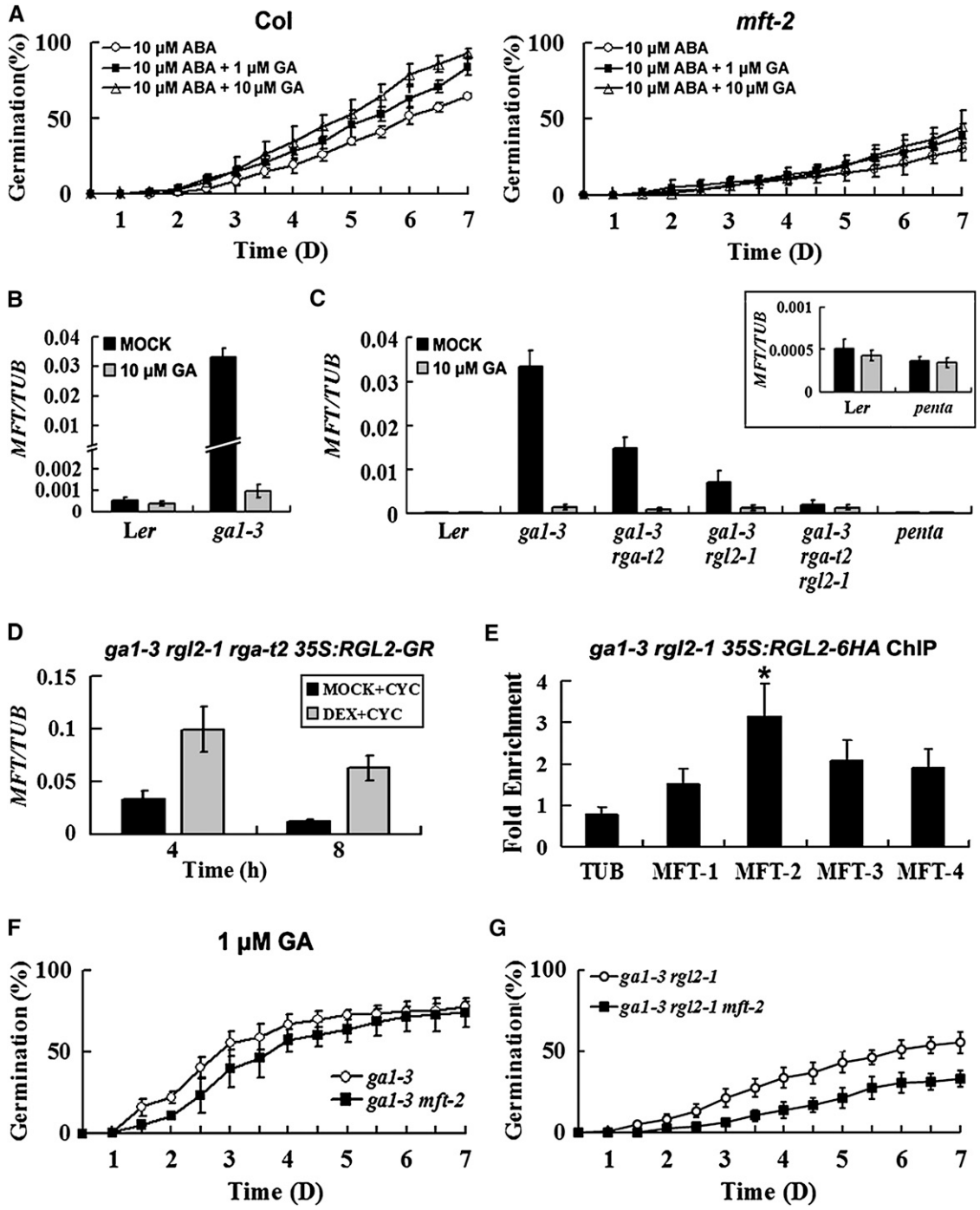

Figure 5. Regulation of *MFT* by GA Is Mediated by DELLA Proteins.

(A) Germination phenotype of the wild type and *mft-2* treated with 10 μM ABA plus different concentrations of GA. Error bars denote SD.

(B) *MFT* expression determined by quantitative real-time PCR in wild-type and *ga1-3* seeds mock treated or treated with 10 μM GA. All germinating seeds were collected 16 h after stratification. Error bars denote SD.

(C) *MFT* expression determined by quantitative real-time PCR in wild-type and various *DELLA* mutant seeds in *ga1-3* background mock treated or treated with 10 μM GA. All germinating seeds were collected 16 h after stratification. *penta* indicates the *ga1-3 gai-t6 rga-t2 rgl1-1 rgl2-1* mutant. Inset shows the comparison of *MFT* expression between the wild type and *penta* mutants. Error bars denote SD.

(D) *MFT* expression determined by quantitative real-time PCR in *ga1-3 rgl2-1 rga-t2 35S:RGL2-GR* seeds. Seeds were treated with 30 μM DEX plus 30 μM cycloheximide (CYC) or MOCK (0.09% ethanol) plus cycloheximide under vacuum for 1 h. They were subsequently washed three times and

gMFT-GFP transgenic lines obtained, 10 lines could rescue the ABA hypersensitivity phenotype of *mft-2*, indicating that the MFT-GFP fusion protein is biologically functional (Figure 6A). MFT-GFP signals in the cells of the radical-hypocotyl transition zone were located in the nucleus, implying that MFT may function as a transcription coregulator that modulates downstream gene expression (Figure 6B). The similar nuclear localization has also been observed in another MFT homolog, FT, which functions in the nucleus to regulate the expression of other flowering genes (Abe et al., 2005; Wigge et al., 2005).

To evaluate how *MFT* affects the expression of other genes during seed germination, we tested a group of ABA marker genes and found that the expression of *RD29A*, *RD29B*, and *Em6* was higher in *mft-2* than in the wild type in response to ABA (see Supplemental Figure 10 online). Since *Em6* is a known direct downstream target of *ABI5* (Finkelstein and Lynch, 2000; Lopez-Molina et al., 2002) and *ABI5* expression in the radicle overlaps with *MFT* expression in response to ABA (Piskurewicz et al., 2008) (Figure 2C), we asked if *MFT* regulates *ABI5*, thus affecting *Em6* expression. We found that in germinating seeds, *ABI5* expression in *mft-2* was higher than in the wild type in response to exogenous ABA (Figure 6C). Furthermore, in situ hybridization revealed higher *ABI5* expression levels in the radicle of *mft-2* than in the wild type (Figure 6D). This suggests that *MFT* negatively regulates *ABI5* in the radicle of germinating seeds in response to ABA. To test whether MFT is directly associated with the *ABI5* promoter, we created *mft-2 gMFT-HA* transgenic plants that fully rescued the *mft-2* phenotype (Figure 6E). ChIP assays showed the enrichment of MFT-HA at the promoter region near the ABI5-2 fragment (Figures 6F and 6G), whereas no binding was observed on the *ABI3* promoter (see Supplemental Figure 11 online), suggesting that *MFT* antagonizes ABA signaling by directly repressing *ABI5*. This was supported by the expression analysis showing that *ABI3* upregulation of *ABI5* in *35S:ABI3-6HA* was enhanced in *mft-2* in response to ABA (Figure 6H). Furthermore, *abi5-1 mft-2* double mutants could fully rescue the low germination defects of *mft-2* in response to ABA.

DISCUSSION

MFT Expression Is Mediated by ABA and GA Signaling Pathways

Seed germination starts with the uptake of water by the dry seed and terminates with the visible penetration of the structures surrounding the embryo by the embryonic axis (Bewley, 1997). This process is governed by two major counteracting phytohormones, ABA and GA, in response to various environmental factors. As these two hormones act through a complex crosstalk rather than through independent pathways (Kucera et al., 2005), integration of their mutual interaction is critical for a plant to make a decision on whether it should initiate germination. The DELLA protein RGL2 and ABA biosynthesis are two known factors involved in this integration, in which they promote each other via a positive feedback regulatory loop (Piskurewicz et al., 2008). In this study, we show that *MFT* responds to ABA and GA signaling to modulate *ABI5* expression in the radicle of the embryo, thus specifically regulating the timing of seed germination in response to environmental factors (Figure 7).

Several pieces of evidence suggest that *MFT* serves as a convergence point of ABA and GA signaling pathways during seed germination. First, ABI5, which represses seed germination in response to ABA and GA (Piskurewicz et al., 2008), directly upregulates *MFT* in the radical-hypocotyl transition zone of the embryo. In the absence of *ABI5*, upregulation of *MFT* in response to ABA is abolished, while overexpression of *ABI5* increased *MFT* expression. ABI5 binds to the *MFT* promoter region close to the start codon, where there is a single ABRE. Mutation of the G-box in this ABRE abolishes the upregulation of *MFT* expression in the radical-hypocotyl transition zone by increased ABI5 activity. These results strongly suggest that ABI5 specifically regulates *MFT* expression in the radical-hypocotyl transition zone through the G-box in the ABRE near the start codon. It is noteworthy that in *abi5-1*, GUS staining of *MFT(P2)-GUS* in the whole embryo still increased in response to ABA (Figure 4D). This is consistent with the expression analysis showing slightly upregulated *MFT* expression in *abi5-1* in response to ABA (Figure 3A), implying that some other factor(s) act concomitantly with ABI5 to upregulate *MFT* in the ABA pathway. In addition to ABI5, there are other four bZIP ABRE binding factors (ABFs) that recognize the G-box motif (Choi et al., 2000). Among them, ABF3 has been shown to function redundantly with ABI5 during seed germination (Finkelstein et al., 2005) and thus might be another potential upstream regulator of *MFT*.

Second, ABI3, another key transcription factor in the ABA pathway, also directly represses *MFT*. *MFT* is downregulated in *35S:ABI3* germinating seeds treated with ABA. Furthermore, ChIP assays have shown that the genomic region near the MFT-2 fragment, where several ABREs are located, is associated with ABI3-6HA (Figure 3D). This suggests that *ABI3* plays a role in directly repressing *MFT* in response to ABA during seed germination. Interestingly, *MFT* was dramatically upregulated in *abi3-1* germinating seeds even without ABA treatment (Figures 3A and 4D). We speculate that upregulation of *MFT* in *abi3-1* may partly result from a failure in establishing seed maturation in *abi3-1* (Nambara et al., 1995), which causes a

Figure 5. (continued).

collected 4 and 8 h after sowing on MS medium. Error bars denote SD.

(E) ChIP results showing the binding of RGL2-6HA to the *MFT* promoter. Primers used for the enrichment test are described in Figure 3D. Seeds were sown on MS medium and harvested 16 h after stratification for ChIP assays. A significant difference in comparison with the enrichment of a *TUB2* fragment is indicated with an asterisk ($P < 0.05$, Student's *t* test). Error bars denote SD.

(F) Germination phenotype of *ga1-3* and *ga1-3 mft-2* treated with 1 μM GA. Error bars denote SD.

(G) Germination phenotype of *ga1-3 rgl2-1* and *ga1-3 rgl2-1 mft-2* in the absence of exogenous GA. Error bars denote SD.

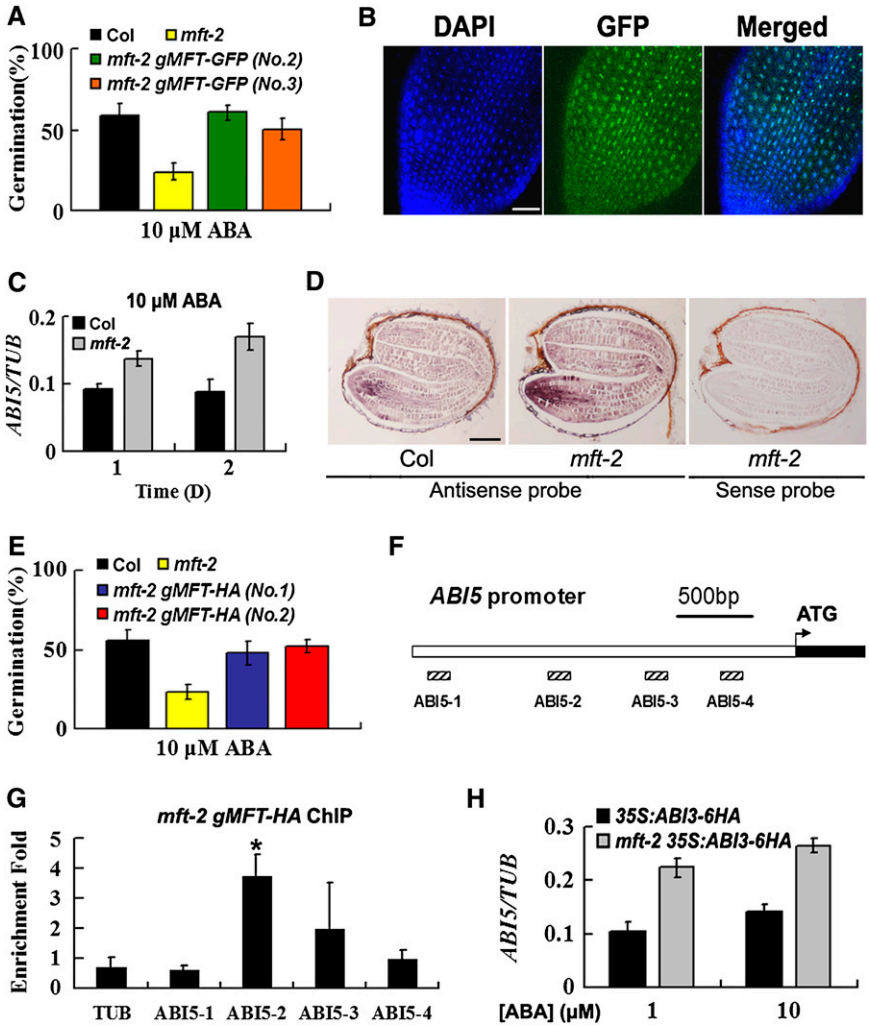

Figure 6. *MFT* Antagonizes ABA Signaling by Directly Repressing *ABI5* during Seed Germination.

(A) Two representative *mft-2 gMFT-GFP* transgenic lines showing rescued germination phenotype in response to 10 μM ABA. The percentage of germination was scored 7 d after stratification. Error bars denote SD.

(B) MFT-GFP localization in the cells of the radical-hypocotyl transition zone. DAPI, fluorescence of 4',6-diamidino-2-phenylindole; Merged, merge of DAPI and GFP. Bar = 50 μm.

(C) Expression of *ABI5* determined by quantitative real-time PCR in wild-type and *mft-2* seeds treated with 10 μM ABA at 1 or 2 d after stratification. Error bars denote SD.

(D) In situ localization of *ABI5* in wild-type and *mft-2* seeds treated with 10 μM ABA. Seeds were collected 24 h after stratification. Bar = 100 μm.

(E) Two representative *mft-2 gMFT-HA* transgenic lines showing rescued germination phenotype in response to 10 μM ABA. The percentage of germination was scored 7 d after stratification. Error bars denote SD.

(F) Schematic diagram of the *ABI5* promoter region. White and black boxes represent the upstream region and part of the first exon, respectively. Hatched boxes represent the DNA fragments amplified in ChIP assays.

(G) ChIP enrichment test showing the binding of MFT-HA to the *ABI5* promoter. Seeds were sown on MS medium supplemented with 10 μM ABA and harvested 24 h after stratification for ChIP assays. A significant difference in comparison with the enrichment of a *TUB2* fragment is indicated with an asterisk ($P < 0.05$, Student's *t* test). Error bars denote SD.

(H) *ABI5* expression determined by quantitative real-time PCR in germinating seeds of *35S:ABI3-6HA* and *mft-2 35S:ABI3-6HA* treated with 1 and 10 μM ABA. Germinating seeds were collected 24 h after stratification. Error bars denote SD.

global change in transcription. In agreement with this idea, *MFT* expression is particularly strong in the whole embryo of *abi3-1* seeds (Figure 4D), which resembles its expression pattern in wild-type immature seeds (see Supplemental Figure 12 online). Thus, the significantly elevated *MFT* expression in *abi3-1* may reflect ABI3 regulation of *MFT* expression in the underdeveloped embryo.

Third, our data suggest that among all the DELLA proteins involved in the regulation of *MFT*, RGL2 is the main one that directly modulates *MFT* expression. When GA levels are low,

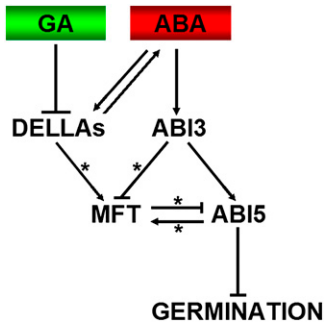

Figure 7. A Proposed Model of Seed Germination Mediated by *MFT*.

ABA regulates *MFT* expression via *ABI3* and *ABI5* with the former acting as a repressor and the latter as a promoter. *MFT* confers negative feedback regulation of the ABA signaling pathway through directly repressing *ABI5*. On the other hand, GA downregulates *MFT* expression and inhibits ABA synthesis via DELLA proteins (i.e., RGL2). Therefore, *MFT* serves as a mediator in response to ABA and GA signals to promote seed germination through constituting a negative feedback regulation of ABA signaling. Asterisks represent direct transcriptional regulation.
[See online article for color version of this figure.]

RGL2 promotes ABA biosynthesis through stimulating the expression of *XERICO*, which encodes a RING-H2 zinc finger factor (Ko et al., 2006; Zentella et al., 2007; Piskurewicz et al., 2008). In turn, an elevation of endogenous ABA levels promotes the mRNA expression of *RGL2* and *ABI5* and the protein expression and activity of ABI5 (Piskurewicz et al., 2008). Thus, direct upregulation of *MFT* by RGL2 allows *MFT* to respond to both GA and ABA pathways when they generate a signal output that does not permit germination under unfavorable environmental conditions.

Negative Feedback Regulation of *ABI5*

ABI5 has been identified as the final and common downstream repressor of seed germination in response to ABA and GA (Piskurewicz et al., 2008). The function of ABI5 is modulated by phosphorylation mediated by SnRK2-type kinases and sumoylation mediated by SUMO E3 ligase (Lopez-Molina et al., 2001; Fujii et al., 2007; Miura et al., 2009). ABI5 prevents seed germination partly by activating a group of *LATE EMBRYOGENESIS ABUNDANT* genes, including *Em1* and *Em6* (Finkelstein and Lynch, 2000; Lopez-Molina et al., 2002), which encode hydrophilic proteins possibly required for desiccation tolerance (Vicient et al., 2000). So far, several upstream regulators of *ABI5* have been reported. *ABI3* functions as an upstream promoter of *ABI5* to regulate the growth arrest of germinating seed (Lopez-Molina et al., 2002). Because *35S:ABI5* could rescue ABA insensitivity of *abi3* during germination, *ABI5* has been suggested as an essential factor acting downstream of *ABI3* and executing an ABA-dependent growth arrest (Lopez-Molina et al., 2002). Genetic analysis has also suggested that *ABF1* and *ABF3* participate in antagonizing *ABI5* expression (Finkelstein et al., 2005). In addition, HY5, a light-signaling mediator, directly activates *ABI5* to integrate light and ABA signaling (Chen et al., 2008).

Here, we show that *MFT* responds to the signals from ABA and GA pathways and generates a negative feedback loop in the ABA pathway by directly repressing *ABI5* (Figure 7). When ABA levels are high, ABI5 directly promotes the expression of *MFT*, which in turn directly represses *ABI5* expression in the radicle of the embryo, thus maintaining the embryo growth potential even under high levels of ABA. Upon ABA treatment, *mft* mutants exhibit enhanced upregulation of *ABI5* in the radicle of the embryo, thus resulting in the ABA hypersensitive phenotype. As MFT protein does not contain any DNA binding domain, there are likely to be other transcription factors involved in guiding the MFT protein to the *ABI5* promoter. A bZIP transcription factor, FD, has been shown to interact with the MFT homolog FT, and such a protein complex participates in activating a floral homeotic gene *APETALLA1* (Abe et al., 2005; Wigge et al., 2005). Identification of the MFT-interacting partner(s) remains as an intriguing subject for future research.

MFT-Like Genes May Have Conserved Function in Plants

The PEBP family is evolutionarily conserved in a wide range of multicellular land plants, and phylogenetic studies of PEBP-like genes in angiosperms have divided them into three main subfamilies, *FT*-like, *TFL1*-like, and *MFT*-like clades (Kobayashi et al., 1999; Carmel-Goren et al., 2003; Chardon and Damerval, 2005; Carmona et al., 2007; Hedman et al., 2009). A recent study on *MFT*-like genes in a basal plant lineage *Physcomitrella patens* (bryophyte) suggested that the MFT-like clade is ancestral to the other two clades (Hedman et al., 2009). In *Arabidopsis*, three PEBP members, *FT*, *TFL1*, and *TWIN SISTER OF FT*, have been shown to regulate flowering time and shoot meristem identity (Bradley et al., 1997; Kardailsky et al., 1999; Kobayashi et al., 1999; Yamaguchi et al., 2005). Although *MFT* shares sequence similarity with *FT* and *TFL1*, its loss-of-function mutant in the Wassilewskija-2 (Ws) ecotype background does not exhibit relevant defects in flowering and meristem development (Yoo et al., 2004), which is consistent with what we have observed in *mft-2* and *mft-3* in Col. A comparison of protein sequences has revealed a critical amino acid residue (Trp) in MFT that differs from Tyr or His in FT or TFL1, respectively, in which this residue is located in a potential ligand binding pocket and determines the protein function as a flowering inducer or repressor (Hanzawa et al., 2005). Notably, this residue is well conserved in most MFT-like proteins (Hedman et al., 2009). Furthermore, almost all MFT-like proteins share another conserved Pro residue near the C terminus, which is absent in FT-like or TFL1-like proteins (Hedman et al., 2009). These observations imply that MFT may have different roles in plant development compared with FT and TFL1.

In this study, we show that *MFT* functions as an antagonistic factor of ABA signaling during seed germination. *MFT* expression is boosted by ABA and inhibited by GA and *MFT* promotes seed germination particularly when ABA levels are elevated under environmental stresses. Like *MFT* expression in *Arabidopsis* (Figures 1A and 1B; see Supplemental Figure 12 online), most of the identified *MFT*-like genes in various plant species show preferential expression in seeds (Chardon and Damerval, 2005; Danilevskaya et al., 2008), implying a highly conserved function

of *MFT*-like genes in seed development across the plant kingdom. Analysis of the genomic sequences of *MFT*-like genes in maize (*Zea mays*) and rice (*Oryza sativa*) revealed that they all contain several ABREs near their coding regions, which is comparable to the ABREs identified in *MFT* in *Arabidopsis* (see Supplemental Figure 13 online). Therefore, it will be interesting and of practical importance to study further whether *MFT*-like genes in other plants have a conserved function in tuning seed sensitivity to ABA, thus modulating the growth potential of the embryo in response to environmental cues.

METHODS

Plant Materials

Arabidopsis thaliana ecotype Col-0 was used in the generation of all transgenic plants. *abi1-1*, *abi2-1*, and *abi3-1* are in the L*er* background; *abi4-1*, *mft-2*, *mft-3*, *aba1-5*, *cyp707a1-1*, and *cyp707a2-1* are in Col background; and *abi5-1* is in the Wassilewskija background. *mft-2* introgressed into L*er* was obtained by three backcrosses of *mft-2* into L*er*. Different combinations of *DELLA* mutants in *ga1-3* background (L*er*) have been described previously (Yu et al., 2004b).

Plant Growth Conditions, Seed Germination Assay, and Stress Treatment

Plants were grown at 22°C under long days (16 h of light/8 h of dark). Dry seeds were collected and stored at a dehumidifier cabinet for at least 2 months before the seed germination test was performed. After-ripened seeds were washed with 70% (v/v) ethanol for 30 s, sterilized with 10% (v/v) commercial Clorox bleach for 15 min, and washed three times with sterile water. Sterilized seeds were subsequently plated on MS medium (Sigma-Aldrich) containing 0.8% (w/v) Bacto Agar (Difco/BD) supplemented with ABA, NaCl, or GA_3. Stock solution of ABA (mixed isomers; Sigma-Aldrich) was in methanol, while GA_3 (Sigma-Aldrich) was in ethanol. Control plates contained equal amounts of the corresponding solvents. Plates were kept at 4°C in darkness for 3 d for stratification and then transferred to a tissue culture room set at 22°C with a 16-h-light/8-h-dark photoperiod. For the germination assay, at least 100 seeds for each genotype were sterilized and sown on MS medium supplemented with or without phytohormones or chemicals. Germination was defined as the first sign of radicle tip emergence and scored daily until the 7th day of the incubation, and the germination results were calculated based on at least three independent experiments. Drought treatment and measurement of transpiration rates were performed as previously described (Kang et al., 2002).

Plasmid Construction

For construct *35S:MFT*, the *MFT* coding region was amplified using primers MFT_P1_PstI (5′-CCCTGCAGATATATATCTCCCTCCCCGC-3′) and MFT_P2_SpeI (5′-CCACTAGTTTTTTGTACTAGCGTCTGCG-3′). The PCR products were digested with *Pst*I and *Spe*I and inserted into the corresponding sites of the pGreen 0229-35S binary vector (Yu et al., 2004a). To construct *MFT(P2)-GUS*, the 1.8-kb *MFT* 5′ upstream sequence was amplified with the primers MFTGUS_P1_HindIII (5′-CCAAGCTTCTACGCGATTGGACGTTGC-3′) and MFTGUS-P5-XmaI (5′-ACCCGGGCGATCAGCGGGGAGGGAGAT-3′). To construct *MFT(P6)-GUS*, the 900-bp *MFT* 5′ upstream sequence was amplified with the primers MFTGUS-P4-HindIII (5′-CCAAGCTTCGATGAATATGCGACCGACC-3′) and MFTGUS-P5-XmaI. The digested PCR products were cloned into pHY107 (Liu et al., 2007). These constructs were mutagenized to produce the mutated ABA response elements (Figure 4A) using the QuikChange II XL site-directed mutagenesis kit (Stratagene). Two *MFT* genomic fragments (*gMFT-P2* and *gMFT-P6*) were used for the complementation test. *gMFT-P2* comprised the 1.8-kb upstream sequence and the 2.1-kb coding sequence plus introns and amplified using the primers MFTGUS_P1_HindIII and MFT_P2'_XmaI (5′-ACCCGGGCTAGCGTCTGCGTGAAGCAGGTTCC-3′). *gMFT-P6* contained the 900-bp upstream sequence and the 2.1-kb coding sequence plus introns and was amplified by MFTGUS-P4-HindIII and MFT_P2'_XmaI. These fragments were digested and inserted into pHY105 (Liu et al., 2007). To construct *gMFT-HA*, a single HA tag was incorporated into pHY105-*gMFT-P2* construct using the primers MFT-inverse-RC (5′-CAGCGAATTATCTAGAACTAGCTAGCGTCTGCGTGAAGCAGGTCC-3′) and gMFT-HA-R (5′-AGCGTAATCTGGAACGTCATATGGATAGCGTCTGCGTGAAGCAGGTTCC-3′) by the mutagenesis PCR method. To construct *35S:ABI3-6HA*, the *ABI3* cDNA was amplified with the primers ABI3-6HA_P1_XhoI (5′-CCCTCGAGCC ACTTCAACGATGAAAAGCTTGCATGTGG-3′) and ABI3-6HA_P2_SpeI (5′-GGACTAGTTTTAACAGTTTGAGAAGTTGGTGAAGCGACCAC-3′). The resulting products were digested by *Spe*I and *Xho*I and cloned into pGreen-35S-6HA to obtain an in-frame fusion of *ABI3-6HA* under the control of 35S promoter (Liu et al., 2008). Similarly, *35S:ABI5-6HA* and *35S:RGL2-6HA* were constructed using the primers ABI5-6HA_P1_XhoI (5′-CCCTCGAGGCAGTTGTTAAATGGTAACTAGAG-3′) and ABI5-6HA_P2_SpeI (5′-GGACTAGTGAGTGGACAACTCGGGTTCCTCATC-3′) and the primers RGL2-EcoRV-F (5′-GGGATATCAACAAGAAAGATGAAGAGAGGATACGGAG-3′) and RGL2-XmaI-R2 (5′-CCCCCCGGGGGCGAGTTTCCACGCCGAGG-3′), respectively.

RNA Extraction and Real-Time PCR

Total RNAs from seeds were extracted using the RNAqueous small-scale phenol-free total RNA isolation kit (Ambion) according to the manufacturer's instructions and reverse transcribed using the SuperScript RT-PCR system (Invitrogen). Quantitative real-time PCR was performed using the Power SYBR Green PCR Master mix (Applied Biosystems) as previously reported (Liu et al., 2007). Gene expression was normalized to the expression of *Tubulin* (*TUB2*). Primers used are listed in Supplemental Table 1 online.

ChIP Assays

For ChIP assays, ~300 mg germinating seeds were fixed for 45 min at 4°C with 1% formaldehyde in MC buffer (10 mM potassium phosphate, pH 7.0, 50 mM NaCl, and 0.1 M sucrose) under vacuum. After adding glycine to a concentration of 150 mM, the fixed seeds were shaken for 20 min at 4°C, washed three times with MC buffer, and homogenized in the reaction buffer (50 mM HEPES, pH 7.5, 150 mM NaCl, 1 mM EDTA, 1% Triton X-100, and 0.1% SDS) supplemented with Protease Inhibitor Cocktail tablets (Roche). The mixture was sonicated to produce DNA fragments between 200 and 1 kb. Ten percent solubilized chromatin was saved as an input control, and the remaining was thereafter incubated with anti-HA agarose beads (Sigma-Aldrich) for 1.5 h at 4°C. Beads were washed twice with IP buffer (50 mM HEPES, pH 7.5, 150 mM KCl, 5 mM $MgCl_2$, 10 μM $ZnSO_4$, 1% Triton X-100, and 0.05% SDS), twice with high-salt IP buffer with the concentration of KCl increased to 500 mM, once with LNDET buffer (0.25 M LiCl, 1% Nonidet P-40, 1% deoxycholate, 1 mM EDTA, and 10 mM Tris, pH 8.0), and once with IP buffer again. Beads were then incubated with the elution buffer (50 mM Tris, pH 8.0, 1% SDS, and 10 mM EDTA) for 30 min at 65°C. The eluted supernatant and the input control that was topped up with the elution buffer to a final volume equal to that of the eluted supernatant were added with NaCl to a final concentration of 200 mM. They were incubated at 65°C for 6 h for reverse cross-linking followed by 40 mM proteinase K treatment for 1 h at 45°C. DNA was then recovered using

the QIAquick PCR purification kit (Qiagen). For each ChIP assay, three independent experiments were performed using seeds collected separately. DNA enrichment was examined by quantitative real-time PCR in triplicates as previously described (Liu et al., 2008). The enrichment of a *TUB2* genomic fragment was used as negative control. Primer pairs used for the ChIP enrichment test are listed in Supplemental Table 1 online.

In Situ Hybridization and GUS Activity Analysis

In situ hybridization was performed as previously reported (Liu et al., 2007). For the synthesis of *MFT* RNA probe, the gene-specific region was amplified using the primers 5′-CCTCTCTGTTTCTCTCTCTCTC-3′ and 5′-AAGTATCTCTTTTCCTCTTGAG-3′. Full-length *ABI5* coding sequence was amplified to synthesize the *ABI5* RNA probe. The PCR products were cloned into pGEM-T Easy vector (Promega) to produce the template for in vitro transcription by DIG RNA labeling kit (Roche). For each MFT-GUS reporter construct, we checked at least 15 independent transgenic lines at the T3 generation. A representative line for each MFT-GUS construct was selected for further analysis. GUS staining was performed as previously described (Yu et al., 2002).

Accession Numbers

Sequence data from this article can be found in the Arabidopsis Genome Initiative or GenBank/EMBL databases under the following accession numbers: *MFT* (At1g18100), *ABI3* (At3g24650), *ABI4* (At2g40220), *ABI5* (At2g36270), *RGL2* (At3g03450), *RD29A* (At5g52310), *RD29B* (At5g52300), At *Em6* (At2g40170), *CRC* (At4g28520), At *2S3* (At4g27160), Os *MFT1* (Os06g0498800), Os *MFT2* (Os01g0111600), *ZCN9* (Eu241925), *ZCN10* (Eu241926), and *ZCN11* (Eu241927).

Supplemental Data

The following materials are available in the online version of this article.

Supplemental Figure 1. Quantification of Endogenous ABA Levels in Wild-Type and *mft-2* Seeds after Imbibition.

Supplemental Figure 2. Postgermination Growth of *mft* Is Not Hypersensitive to ABA Treatment.

Supplemental Figure 3. *mft* Is Not Hypersensitive to Drought Stress.

Supplemental Figure 4. In Situ Localization of *MFT* in Seeds Collected 6 h after Stratification Treated without or with 10 μm ABA.

Supplemental Figure 5. Expression of *MFT*, *RGL2*, *ABI3*, and *ABI5* in Wild-Type, *cyp707a1-1*, and *cyp707a2-1* Seeds after Imbibition.

Supplemental Figure 6. Expression of *MFT*, *ABI3*, *ABI4*, and *ABI5* in Wild-type Seeds after Imbibition.

Supplemental Figure 7. Complementation of *mft-2* by Two *MFT* Genomic Fragments *gMFT-P2* and *gMFT-P6*.

Supplemental Figure 8. A Biologically Active RGL2-GR Fusion.

Supplemental Figure 9. *ABI3* and *ABI5* Expression in Seeds of *ga1-3* Lacking DELLA Proteins That Were Mock Treated or Treated with 10 μM GA.

Supplemental Figure 10. Expression of Several ABA Marker Genes in Wild-Type and *mft-2* in Response to ABA.

Supplemental Figure 11. *ABI3* Promoter Is Not Directly Bound by MFT-HA.

Supplemental Figure 12. GUS Staining Pattern of *MFT(P2)-GUS* in Different Tissues.

Supplemental Figure 13. Promoter Analysis of *MFT*-like Subfamily Genes in *Arabidopsis*, Rice, and Maize.

Supplemental Table 1. Primers Used in This Study.

ACKNOWLEDGMENTS

We thank T. Ito, J. Dinneny, and J. Xu for critical reading of the manuscript, the ABRC for the seeds of *abi1-1*, *abi2-1*, *abi3-1*, *abi4-1*, *abi5-1*, *mft-2*, *mft-3*, and *aba1-5*, and M. Okamoto and E. Nambara for the seeds of *cyp707a1-1* and *cyp707a2-1*. This work was supported by Academic Research Funds T208B3113 from the Ministry of Education, Singapore, and R-154-000-337-112 from the National University of Singapore and intramural research funds from Temasek Life Sciences Laboratory. C.L. was supported by the Singapore Millennium Foundation.

Received November 24, 2009; revised April 18, 2010; accepted May 27, 2010; published June 15, 2010.

REFERENCES

Abe, M., Kobayashi, Y., Yamamoto, S., Daimon, Y., Yamaguchi, A., Ikeda, Y., Ichinoki, H., Notaguchi, M., Goto, K., and Araki, T. (2005). FD, a bZIP protein mediating signals from the floral pathway integrator FT at the shoot apex. Science **309:** 1052–1056.

Bewley, J.D. (1997). Seed germination and dormancy. Plant Cell **9:** 1055–1066.

Bradley, D., Ratcliffe, O., Vincent, C., Carpenter, R., and Coen, E. (1997). Inflorescence commitment and architecture in *Arabidopsis.* Science **275:** 80–83.

Carmel-Goren, L., Liu, Y.S., Lifschitz, E., and Zamir, D. (2003). The *SELF-PRUNING* gene family in tomato. Plant Mol. Biol. **52:** 1215–1222.

Carmona, M.J., Calonje, M., and Martinez-Zapater, J.M. (2007). The *FT/TFL1* gene family in grapevine. Plant Mol. Biol. **63:** 637–650.

Chardon, F., and Damerval, C. (2005). Phylogenomic analysis of the PEBP gene family in cereals. J. Mol. Evol. **61:** 579–590.

Chen, H., Zhang, J., Neff, M.M., Hong, S.W., Zhang, H., Deng, X.W., and Xiong, L. (2008). Integration of light and abscisic acid signaling during seed germination and early seedling development. Proc. Natl. Acad. Sci. USA **105:** 4495–4500.

Choi, H., Hong, J., Ha, J., Kang, J., and Kim, S.Y. (2000). ABFs, a family of ABA-responsive element binding factors. J. Biol. Chem. **275:** 1723–1730.

Danilevskaya, O.N., Meng, X., Hou, Z., Ananiev, E.V., and Simmons, C.R. (2008). A genomic and expression compendium of the expanded PEBP gene family from maize. Plant Physiol. **146:** 250–264.

Dill, A., and Sun, T. (2001). Synergistic derepression of gibberellin signaling by removing RGA and GAI function in *Arabidopsis thaliana.* Genetics **159:** 777–785.

Ezcurra, I., Ellerstrom, M., Wycliffe, P., Stalberg, K., and Rask, L. (1999). Interaction between composite elements in the napA promoter: Both the B-box ABA-responsive complex and the RY/G complex are necessary for seed-specific expression. Plant Mol. Biol. **40:** 699–709.

Ezcurra, I., Wycliffe, P., Nehlin, L., Ellerstrom, M., and Rask, L. (2000). Transactivation of the *Brassica napus* napin promoter by ABI3 requires interaction of the conserved B2 and B3 domains of ABI3 with different *cis*-elements: B2 mediates activation through an ABRE, whereas B3 interacts with an RY/G-box. Plant J. **24:** 57–66.

Finkelstein, R.R. (1994). Mutations at two new *Arabidopsis* ABA response loci are similar to the *abi3* mutations. Plant J. **5:** 765–771.

Finkelstein, R.R., Gampala, S.S., and Rock, C.D. (2002). Abscisic acid signaling in seeds and seedlings. Plant Cell **14**(Suppl): S15–S45.

Finkelstein, R.R., Gampala, S.S., Lynch, T.J., Thomas, T.L., and Rock, C.D. (2005). Redundant and distinct functions of the ABA response loci *ABA-INSENSITIVE(ABI)5* and *ABRE-BINDING FACTOR (ABF)3.* Plant Mol. Biol. **59:** 253–267.

Finkelstein, R.R., and Lynch, T.J. (2000). The *Arabidopsis* abscisic acid response gene *ABI5* encodes a basic leucine zipper transcription factor. Plant Cell **12:** 599–609.

Fujii, H., Verslues, P.E., and Zhu, J.K. (2007). Identification of two protein kinases required for abscisic acid regulation of seed germination, root growth, and gene expression in *Arabidopsis.* Plant Cell **19:** 485–494.

Giraudat, J., Hauge, B.M., Valon, C., Smalle, J., Parcy, F., and Goodman, H.M. (1992). Isolation of the *Arabidopsis ABI3* gene by positional cloning. Plant Cell **4:** 1251–1261.

Gubler, F., Millar, A.A., and Jacobsen, J.V. (2005). Dormancy release, ABA and pre-harvest sprouting. Curr. Opin. Plant Biol. **8:** 183–187.

Hanzawa, Y., Money, T., and Bradley, D. (2005). A single amino acid converts a repressor to an activator of flowering. Proc. Natl. Acad. Sci. USA **102:** 7748–7753.

Hedman, H., Kallman, T., and Lagercrantz, U. (2009). Early evolution of the MFT-like gene family in plants. Plant Mol. Biol. **70:** 359–369.

Kang, J.Y., Choi, H.I., Im, M.Y., and Kim, S.Y. (2002). Arabidopsis basic leucine zipper proteins that mediate stress-responsive abscisic acid signaling. Plant Cell **14:** 343–357.

Kardailsky, I., Shukla, V.K., Ahn, J.H., Dagenais, N., Christensen, S.K., Nguyen, J.T., Chory, J., Harrison, M.J., and Weigel, D. (1999). Activation tagging of the floral inducer *FT.* Science **286:** 1962–1965.

Kim, S.Y., Chung, H.J., and Thomas, T.L. (1997). Isolation of a novel class of bZIP transcription factors that interact with ABA-responsive and embryo-specification elements in the *Dc3* promoter using a modified yeast one-hybrid system. Plant J. **11:** 1237–1251.

Kim, S.Y., Ma, J., Perret, P., Li, Z., and Thomas, T.L. (2002). Arabidopsis ABI5 subfamily members have distinct DNA-binding and transcriptional activities. Plant Physiol. **130:** 688–697.

Ko, J.H., Yang, S.H., and Han, K.H. (2006). Upregulation of an Arabidopsis RING-H2 gene, *XERICO*, confers drought tolerance through increased abscisic acid biosynthesis. Plant J. **47:** 343–355.

Kobayashi, Y., Kaya, H., Goto, K., Iwabuchi, M., and Araki, T. (1999). A pair of related genes with antagonistic roles in mediating flowering signals. Science **286:** 1960–1962.

Koornneef, M., Bentsink, L., and Hilhorst, H. (2002). Seed dormancy and germination. Curr. Opin. Plant Biol. **5:** 33–36.

Koornneef, M., Reuling, G., and Karssen, C.M. (1984). The isolation and characterization of abscisic acid-insensitive mutants of *Arabidopsis thaliana.* Physiol. Plant. **61:** 377–383.

Kucera, B., Cohn, M.A., and Leubner-Metzger, G. (2005). Plant hormone interactions during seed dormancy release and germination. Seed Sci. Res. **15:** 281–307.

Lee, S., Cheng, H., King, K.E., Wang, W., He, Y., Hussain, A., Lo, J., Harberd, N.P., and Peng, J. (2002). Gibberellin regulates *Arabidopsis* seed germination via *RGL2*, a *GAI*/*RGA*-like gene whose expression is up-regulated following imbibition. Genes Dev. **16:** 646–658.

Leon-Kloosterziel, K.M., Gil, M.A., Ruijs, G.J., Jacobsen, S.E., Olszewski, N.E., Schwartz, S.H., Zeevaart, J.A., and Koornneef, M. (1996). Isolation and characterization of abscisic acid-deficient *Arabidopsis* mutants at two new loci. Plant J. **10:** 655–661.

Leung, J., and Giraudat, J. (1998). Abscisic acid signal transduction. Annu. Rev. Plant Physiol. Plant Mol. Biol. **49:** 199–222.

Liu, C., Chen, H., Er, H.L., Soo, H.M., Kumar, P.P., Han, J.H., Liou, Y.C., and Yu, H. (2008). Direct interaction of *AGL24* and *SOC1* integrates flowering signals in *Arabidopsis.* Development **135:** 1481–1491.

Liu, C., Zhou, J., Bracha-Drori, K., Yalovsky, S., Ito, T., and Yu, H. (2007). Specification of *Arabidopsis* floral meristem identity by repression of flowering time genes. Development **134:** 1901–1910.

Lopez-Molina, L., Mongrand, S., and Chua, N.H. (2001). A postgermination developmental arrest checkpoint is mediated by abscisic acid and requires the ABI5 transcription factor in *Arabidopsis.* Proc. Natl. Acad. Sci. USA **98:** 4782–4787.

Lopez-Molina, L., Mongrand, S., McLachlin, D.T., Chait, B.T., and Chua, N.H. (2002). ABI5 acts downstream of ABI3 to execute an ABA-dependent growth arrest during germination. Plant J. **32:** 317–328.

Miura, K., Lee, J., Jin, J.B., Yoo, C.Y., Miura, T., and Hasegawa, P.M. (2009). Sumoylation of ABI5 by the *Arabidopsis* SUMO E3 ligase SIZ1 negatively regulates abscisic acid signaling. Proc. Natl. Acad. Sci. USA **106:** 5418–5423.

Muller, K., Tintelnot, S., and Leubner-Metzger, G. (2006). Endosperm-limited Brassicaceae seed germination: Abscisic acid inhibits embryo-induced endosperm weakening of *Lepidium sativum* (cress) and endosperm rupture of cress and *Arabidopsis thaliana.* Plant Cell Physiol. **47:** 864–877.

Nambara, E., Keith, K., McCourt, P., and Naito, S. (1995). A regulatory role for the *ABI3* gene in the establishment of embryo maturation in *Arabidopsis thaliana.* Development **121:** 629–636.

Nambara, E., and Marion-Poll, A. (2005). Abscisic acid biosynthesis and catabolism. Annu. Rev. Plant Biol. **56:** 165–185.

Ogawa, M., Hanada, A., Yamauchi, Y., Kuwahara, A., Kamiya, Y., and Yamaguchi, S. (2003). Gibberellin biosynthesis and response during Arabidopsis seed germination. Plant Cell **15:** 1591–1604.

Okamoto, M., Kuwahara, A., Seo, M., Kushiro, T., Asami, T., Hirai, N., Kamiya, Y., Koshiba, T., and Nambara, E. (2006). CYP707A1 and CYP707A2, which encode abscisic acid 8'-hydroxylases, are indispensable for proper control of seed dormancy and germination in Arabidopsis. Plant Physiol. **141:** 97–107.

Olszewski, N., Sun, T.P., and Gubler, F. (2002). Gibberellin signaling: Biosynthesis, catabolism, and response pathways. Plant Cell **14** (suppl.): S61–S80.

Peng, J., and Harberd, N.P. (1997). Gibberellin deficiency and response mutations suppress the stem elongation phenotype of phytochrome-deficient mutants of Arabidopsis. Plant Physiol. **113:** 1051–1058.

Piskurewicz, U., Jikumaru, Y., Kinoshita, N., Nambara, E., Kamiya, Y., and Lopez-Molina, L. (2008). The gibberellic acid signaling repressor RGL2 inhibits *Arabidopsis* seed germination by stimulating abscisic acid synthesis and ABI5 activity. Plant Cell **20:** 2729–2745.

Schopfer, P., and Plachy, C. (1985). Control of seed germination by abscisic acid: III. Effect on embryo growth potential (minimum turgor pressure) and growth coefficient (cell wall extensibility) in *Brassica napus* L. Plant Physiol. **77:** 676–686.

Tyler, L., Thomas, S.G., Hu, J., Dill, A., Alonso, J.M., Ecker, J.R., and Sun, T.P. (2004). DELLA proteins and gibberellin-regulated seed germination and floral development in Arabidopsis. Plant Physiol. **135:** 1008–1019.

Vicient, C.M., Hull, G., Guilleminot, J., Devic, M., and Delseny, M. (2000). Differential expression of the *Arabidopsis* genes coding for Em-like proteins. J. Exp. Bot. **51:** 1211–1220.

Wen, C.K., and Chang, C. (2002). Arabidopsis *RGL1* encodes a negative regulator of gibberellin responses. Plant Cell **14:** 87–100.

Wigge, P.A., Kim, M.C., Jaeger, K.E., Busch, W., Schmid, M., Lohmann, J.U., and Weigel, D. (2005). Integration of spatial and temporal information during floral induction in *Arabidopsis.* Science **309:** 1056–1059.

Wilson, R.N., Heckman, J.W., and Somerville, C.R. (1992). Gibberellin is required for flowering in *Arabidopsis thaliana* under short days. Plant Physiol. **100:** 403–408.

Xiong, L., Schumaker, K.S., and Zhu, J.K. (2002). Cell signaling during cold, drought, and salt stress. Plant Cell **14** (Suppl): S165–S183.

Xiong, L., and Zhu, J.K. (2003). Regulation of abscisic acid biosynthesis. Plant Physiol. **133:** 29–36.

Yamaguchi, A., Kobayashi, Y., Goto, K., Abe, M., and Araki, T. (2005). *TWIN SISTER OF FT* (*TSF*) acts as a floral pathway integrator redundantly with *FT.* Plant Cell Physiol. **46:** 1175–1189.

Yoo, S.Y., Kardailsky, I., Lee, J.S., Weigel, D., and Ahn, J.H. (2004). Acceleration of flowering by overexpression of *MFT* (*MOTHER OF FT AND TFL1*). Mol. Cells **17:** 95–101.

Yu, H., Ito, T., Wellmer, F., and Meyerowitz, E.M. (2004a). Repression of AGAMOUS-LIKE 24 is a crucial step in promoting flower development. Nat. Genet. **36:** 157–161.

Yu, H., Ito, T., Zhao, Y., Peng, J., Kumar, P., and Meyerowitz, E.M. (2004b). Floral homeotic genes are targets of gibberellin signaling in flower development. Proc. Natl. Acad. Sci. USA **101:** 7827–7832.

Yu, H., Xu, Y., Tan, E.L., and Kumar, P.P. (2002). AGAMOUS-LIKE 24, a dosage-dependent mediator of the flowering signals. Proc. Natl. Acad. Sci. USA **99:** 16336–16341.

Zentella, R., Zhang, Z.L., Park, M., Thomas, S.G., Endo, A., Murase, K., Fleet, C.M., Jikumaru, Y., Nambara, E., Kamiya, Y., and Sun, T.P. (2007). Global analysis of DELLA direct targets in early gibberellin signaling in *Arabidopsis.* Plant Cell **19:** 3037–3057.

Zhang, X., Garreton, V., and Chua, N.H. (2005). The AIP2 E3 ligase acts as a novel negative regulator of ABA signaling by promoting ABI3 degradation. Genes Dev. **19:** 1532–1543.